



# A NEW ELECTRON DRIFT-KINETIC EQUATION SOLVER FOR COUPLED NEOCLASSICAL-MAGNETOHYDRODYNAMIC SIMULATIONS

B.C. LYONS (PPPL), J.J. RAMOS (MIT PSFC), S.C. JARDIN (PPPL)

“RECENT STUDIES OF EXTENDED MHD AND MHD SIMULATIONS”

US-JAPAN JIFT WORKSHOP

DENVER, CO

SUNDAY, NOVEMBER 10, 2013

# Acknowledgements

- This work has been supported by
  - ▣ the U.S. Department of Energy under grant nos. DEFC02-08ER54969 and DEAC02-09CH11466 and the SciDAC Center for Extended Magnetohydrodynamic Modeling (CEMM).
  - ▣ an award from the Department of Energy (DOE) Office of Science Graduate Fellowship Program (DOE SCGF). The DOE SCGF Program was made possible in part by the American Recovery and Reinvestment Act of 2009. The DOE SCGF program is administered by the Oak Ridge Institute for Science and Education for the DOE. ORISE is managed by Oak Ridge Associated Universities (ORAU) under DOE contract number DE-AC05-06OR23100. All opinions expressed in this presentation are the author's and do not necessarily reflect the policies and views of DOE, ORAU, or ORISE.

# Neoclassical tearing mode modeling

3

- NTM stability place a severe limit on maximum  $\beta$
- Most common cause of disruptions on JET<sup>1</sup>
- High-fidelity simulations required for prediction, control, avoidance, and understanding of NTMs
  - ▣ Especially important for ITER operation, in which very few disruptions can be tolerated<sup>2</sup>
- NTMs incorporate a lot of physics
  - ▣ Cause: Neoclassical kinetic theory (bootstrap current)
  - ▣ Effect: MHD destabilization (island growth)
  - ▣ Requires a hybrid model

<sup>1</sup> P.C. de Vries, et al., Nucl. Fusion **51**, 053018 (2011)

<sup>2</sup> T.C. Hender, et al., Nucl. Fusion **47**, S128-S202 (2007)

# Framework for hybrid solver

4

- Use existing MHD time-evolution code (e.g., M3D-C<sup>1</sup>, NIMROD)
- Desirable traits for neoclassical drift–kinetic equation (DKE) solver
  - ▣ Three-dimensional toroidal geometry
    - Study nonaxisymmetric geometries with magnetic islands
  - ▣ Full Fokker-Planck-Landau collision operator
    - Use of model collision operators can lead to errors of 5%-10%<sup>3</sup>
  - ▣ Continuum model
    - Good convergence properties, especially for long times
    - Straight-forward coupling to MHD solvers
    - Potentially more computationally efficient than PIC

<sup>3</sup> E.A. Belli and J. Candy, Plasma Phys. Control. Fusion **54**, 015015 (2012)

# Ramos Form of DKE

5

- J.J. Ramos (Phys. Plasmas 2010 & 2011) provides analytic framework for a neoclassical solver appropriate for core plasma instability simulations
- DKE evolves  $f_{NM_s}$ , difference between full distribution function and shifting Maxwellian (similar to delta-f)
- Small parameters for high-temperature fusion plasmas

$$\delta \sim \rho_i/L \ll 1 \quad \nu_* \sim L/\lambda_{\text{mfp}} \sim \delta$$

- Important properties:
  - Maintained to collisional inverse timescale of  $O(\delta^3 v_{the}/L)$ 
    - Conventional neoclassical banana regime for electrons
  - Velocity  $w$  referenced to each species' macroscopic flow
  - Perturbed distribution function carries no density, parallel momentum, or kinetic energy

# Overview of new code

6

- NIES code<sup>4</sup> successfully solved axisymmetric Ramos DKEs to zeroth order in collisionality
- We'll retain axisymmetric geometry for now
- Want to solve the full Ramos DKE without further expansions in collisionality
  - ▣ Extends result to first-order in collisionality
  - ▣ Allows solution to vary poloidally
  - ▣ Solves for particles' distribution functions in both trapped and passing regions
- Will couple directly to MHD equations

<sup>3</sup> B.C Lyons, S.C. Jardin and J.J. Ramos, Phys. Plasma 19, 082515 (2012)

# Extended MHD equations

7

□ Besides Maxwell's and continuity eqs., we have:

▣ Ohm's Law

$$\mathbf{E} + \mathbf{u} \times \mathbf{B} = \frac{1}{en} \mathbf{F}_e^{coll} + \frac{1}{en} \left\{ \mathbf{J} \times \mathbf{B} - \nabla p_e - \nabla \cdot \left[ (p_{e\parallel} - p_{e\perp}) \left( \mathbf{b}\mathbf{b} - \frac{\hat{\mathbf{I}}}{3} \right) \right] \right\}$$

▣ Momentum evolution

$$nm_i \left( \frac{\partial \mathbf{u}}{\partial t} + \mathbf{u} \cdot \nabla \mathbf{u} \right) + \nabla p - \mathbf{J} \times \mathbf{B} + \nabla \cdot \hat{\mathbf{\Pi}}_{GV} + \nabla \cdot \left[ (p_{\parallel} - p_{\perp}) \left( \mathbf{b}\mathbf{b} - \frac{\hat{\mathbf{I}}}{3} \right) \right] = 0$$

▣ Pressure evolution

$$\frac{3}{2} \left[ \frac{\partial p_e}{\partial t} + \nabla \cdot (p_e \mathbf{u}_e) \right] + p_e \nabla \cdot \mathbf{u}_e + \nabla \cdot \left( q_{e\parallel} \mathbf{b} + \frac{5nT_e}{2eB} \mathbf{b} \times \nabla T_e \right) - G_e^{coll} = 0$$

$$\begin{aligned} \frac{3}{2} \left[ \frac{\partial p_i}{\partial t} + \nabla \cdot (p_i \mathbf{u}_i) \right] + p_i \nabla \cdot \mathbf{u}_i + (p_{i\parallel} - p_{i\perp}) \left( \mathbf{b}\mathbf{b} - \frac{\hat{\mathbf{I}}}{3} \right) : \nabla \mathbf{u}_i \\ + \nabla \cdot (q_{i\parallel} \mathbf{b} - \mathbf{q}_{i\perp}) - G_i^{coll} = 0 \end{aligned}$$

# Required Moments for Closure

8

- Pressure Anisotropy

$$p_{s\parallel} - p_{s\perp} = \frac{1}{2} m_s \int d^3 w \left( 3w_{\parallel}^2 - w^2 \right) f_{NM_s}$$

- Parallel Heat Flux

$$q_{s\parallel} = \frac{1}{2} m_s \int d^3 w w^2 w_{\parallel} f_{NM_s}$$

- Collisional Friction Force

$$\mathbf{F}_e^{coll} = m_e \int d^3 w \mathbf{w} C_{ei} [f_{Me} + f_{NMe}, f_{Mi}]$$

- Collisional Heat Sources

$$G_i^{coll} = -G_e^{coll} + \frac{1}{en} \mathbf{J} \cdot \mathbf{F}_e^{coll} = \frac{2\nu_e n m_e}{(2\pi)^{1/2} m_i} (T_e - T_i)$$

- All of these moments are given by the solution to appropriate DKEs
  - ▣ We'll only consider the electron DKE here



# Electron drift-kinetic equation

9

$$\begin{aligned}
 & \frac{\partial f_{NM_e}}{\partial t} + wy \mathbf{b} \cdot \nabla f_{NM_e} - \frac{1}{2} w (1 - y^2) \mathbf{b} \cdot \nabla \ln B \frac{\partial f_{NM_e}}{\partial y} = \langle C_{ee} + C_{ei} \rangle \\
 & + \left\{ \frac{wy}{nT_e} \mathbf{b} \cdot \left[ \frac{2}{3} \nabla (p_{e\parallel} - p_{e\perp}) - (p_{e\parallel} - p_{e\perp}) \nabla \ln B - \mathbf{F}_e^{coll} \right] \right. \\
 & + P_2(y) \frac{w^2}{3v_{the}^2} (\nabla \cdot \mathbf{u}_e - 3\mathbf{b} \cdot [\mathbf{b} \cdot \nabla \mathbf{u}_e]) + \frac{1}{3nT_e} \left( \frac{w^2}{v_{the}^2} - 3 \right) \nabla \cdot (q_{e\parallel} \mathbf{b}) \\
 & \left. + \frac{1}{3m_e \Omega_e} \left[ \frac{1}{2} P_2(y) \frac{w^2}{v_{the}^2} \left( \frac{w^2}{v_{the}^2} - 5 \right) + \frac{w^4}{v_{the}^4} - 10 \frac{w^2}{v_{the}^2} + 15 \right] (\mathbf{b} \times \nabla \ln B) \cdot \nabla T_e \right\} f_{Me}
 \end{aligned}$$

- Assumes equal ion & electron temperatures
- Axisymmetric 4D phase space
  - ▣  $\tilde{\psi}$  denotes a flux surface,  $\theta$  is the poloidal angle
  - ▣  $w$  is the total velocity,  $y = \cos \chi$  is cosine of the pitch angle
  - ▣ Density, temperatures, and pressures are flux functions

# Electron Collision Operator

10

□ Fokker-Planck-Landau form used

$$\begin{aligned} \langle C_{ee} + C_{ei} \rangle = & \nu_{De}(w) \mathcal{L}[f_{NMe}] + \frac{\nu_e v_{the}^3}{w^2} \frac{\partial}{\partial w} \left\{ \xi_e \left[ w \frac{\partial f_{NMe}}{\partial w} + \frac{w^2}{v_{the}^2} f_{NMe} \right] + \xi_i \left[ w \frac{\partial f_{NMe}}{\partial w} + \frac{m_e w^2}{m_i v_{thi}^2} f_{NMe} \right] \right\} \\ & + \frac{\nu_e v_{the}}{n} f_{Me} \left( 4\pi v_{the}^2 f_{NMe} - \Phi_e[f_{NMe}] + \frac{w^2}{v_{the}^2} \frac{\partial^2 \Psi_e[f_{NMe}]}{\partial w^2} \right) + \nu_e f_{Me} \frac{v_{the}}{v_{thi}^2} \frac{\mathbf{b} \cdot \mathbf{J}}{en} \xi_i y \end{aligned}$$

where

$$\begin{aligned} \nu_{De}(w) = \frac{\nu_e v_{the}^3}{w^3} [\varphi_e - \xi_e + \varphi_i - \xi_i] \quad \mathcal{L}[f] = \frac{1}{2} \frac{\partial}{\partial y} \left[ (1 - y^2) \frac{\partial f}{\partial y} \right] \\ \varphi_s = \varphi \left( x = \frac{w}{v_{ths}} \right) = \frac{2}{\sqrt{2\pi}} \int_0^x \exp(-t^2/2) dt \quad \xi_s = \xi \left( x = \frac{w}{v_{ths}} \right) = \frac{1}{x^2} \left[ \varphi(x) - \frac{2x}{\sqrt{2\pi}} \exp(-x^2/2) \right] \end{aligned}$$

□ Poisson equations for the Rosenbluth potentials

$$\frac{\partial}{\partial w} \left( w^2 \frac{\partial \Phi_e}{\partial w} \right) + \frac{\partial}{\partial y} \left[ (1 - y^2) \frac{\partial \Phi_e}{\partial y} \right] = -4\pi w^2 f_{NMe}$$

$$\frac{\partial}{\partial w} \left( w^2 \frac{\partial \Psi_e}{\partial w} \right) + \frac{\partial}{\partial y} \left[ (1 - y^2) \frac{\partial \Psi_e}{\partial y} \right] = w^2 \Phi_s$$

# Time advancement of Electron DKE

11

$$\begin{aligned}
 & \frac{f_{NM_e}^{n+1}}{\Delta t} - wy \frac{\psi_0}{\mathcal{J}B} \frac{\partial f_{NM_e}^{n+1}}{\partial \theta} + \frac{1}{2} w (1 - y^2) \frac{\psi_0}{\mathcal{J}B^2} \frac{\partial B}{\partial \theta} \frac{\partial f_{NM_e}^{n+1}}{\partial y} - \left[ \langle C_{ee} + C_{ei} \rangle - \nu_e f_{Me} \frac{v_{the}}{v_{thi}^2} \frac{J_{\parallel}}{en} \xi_{iy} \right]^{n+1} \\
 &= \frac{f_{NM_e}^n}{\Delta t} - \frac{1}{3nT_e} \left( \frac{w^2}{v_{the}^2} - 3 \right) f_{Me} \frac{\psi_0}{\mathcal{J}B} \frac{\partial}{\partial \theta} \left( \frac{q_{e\parallel}^n}{B} \right) \\
 & - \frac{wy}{nT_e} f_{Me} \left\{ \frac{2}{3} \frac{\psi_0}{\mathcal{J}B} \frac{\partial}{\partial \theta} (p_{e\parallel} - p_{e\perp})^n - \frac{\psi_0}{\mathcal{J}B^2} \frac{\partial B}{\partial \theta} (p_{e\parallel} - p_{e\perp})^n + \left[ F_{e\parallel}^{coll} - \frac{2m_e \nu_e}{3\sqrt{2\pi e}} J_{\parallel} \right]^n \right\} \\
 & + \left\{ P_2(y) \frac{w^2}{3v_{the}^2} (\nabla \cdot \mathbf{u}_e - 3\mathbf{b} \cdot [\mathbf{b} \cdot \nabla \mathbf{u}_e]) + \nu_e \frac{v_{the}}{v_{thi}^2} \frac{J_{\parallel}}{en} \xi_{iy} - \frac{2}{3\sqrt{2\pi}} \nu_e \frac{w}{v_{the}^2} \frac{J_{\parallel}}{en} y \right\} f_{Me} \\
 & - \frac{1}{3m_e \Omega_e} f_{Me} \left[ \frac{1}{2} P_2(y) \frac{w^2}{v_{the}^2} \left( \frac{w^2}{v_{the}^2} - 5 \right) + \frac{w^4}{v_{the}^4} - 10 \frac{w^2}{v_{the}^2} + 15 \right] \frac{I\psi_0}{\mathcal{J}B^2} \frac{\partial B}{\partial \theta} \frac{dT_e}{d\psi}
 \end{aligned}$$

- Implicit, homogeneous convective and collision operator terms
- Explicit, homogeneous moment terms
  - ▣ No stability constraints expected since these are integrals over the solution
  - ▣ Predictor-corrector option available, but no substantial effect observed
- Inhomogeneous drive terms

# Expansions in DKE

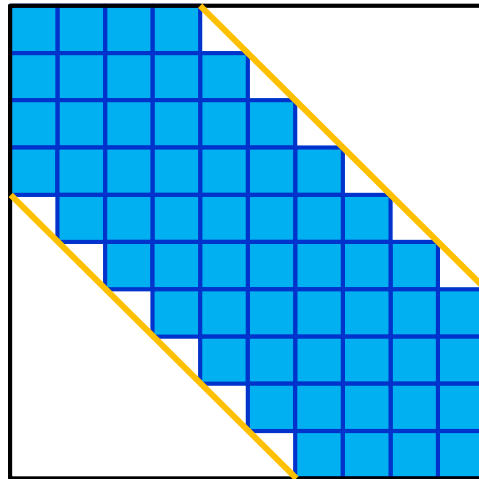
12

- Velocity
  - ▣ Finite elements for  $w$ 
    - Hermite cubics
    - Cubic B-splines
- Pitch angle
  - ▣ Legendre polynomials in  $y = \cos \chi$
  - ▣ May try finite elements soon as well
- Configuration Space
  - ▣ Fourier modes in  $\theta$
  - ▣  $\psi$  is just a parameter (each flux surface treated locally)
  - ▣ May try finite elements in  $\theta$  or in  $(R, Z)$

# DKE Solution Method

13

- Poisson equations for Rosenbluth potentials solved simultaneously with DKE at each time step
- Galerkin method creates a block diagonal matrix in  $w$



- Each block contains information on  $y$  and  $\theta$  derivatives
- Two solver options implemented
  - ▣ Sparse banded matrix using ScaLAPACK
  - ▣ SuperLU via PETSc

# Timescales

14

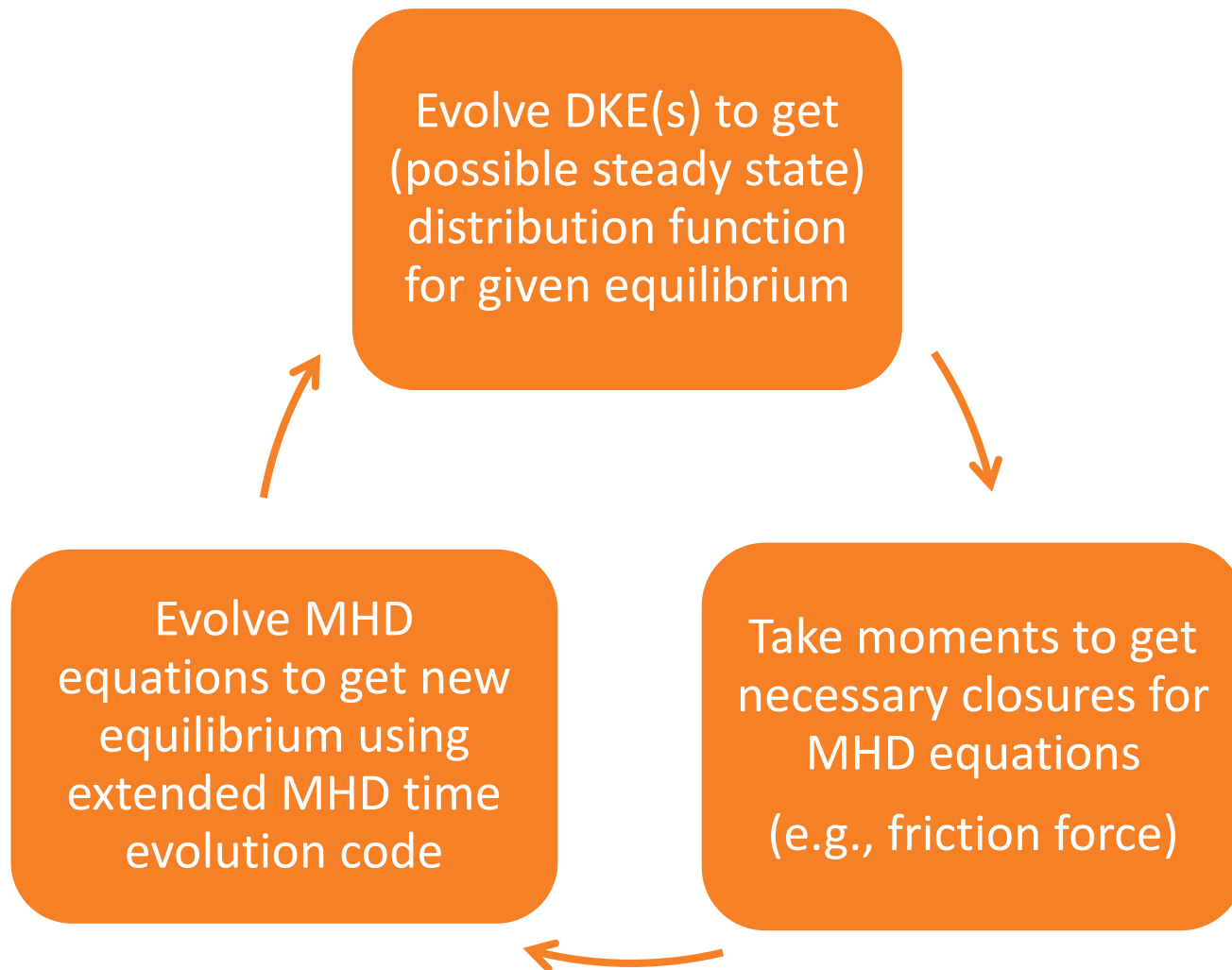
Machine	$n$ ( $\text{m}^{-3}$ )	$T$ (keV)	$B$ (T)	$a$ (m)	$R$ (m)
LTX	$3.15 \times 10^{19}$	0.2	0.34	0.26	0.4
NSTX	$9.04 \times 10^{19}$	1	0.45	0.65	0.85
DIID-D	$1.13 \times 10^{20}$	5	2.1	0.65	1.67
ITER	$1.19 \times 10^{20}$	20	5.3	2.0	6.2

Machine	$\tau_{Alfven}$ (s)	$\tau_{e,conv}$ (s)	$\tau_{i,conv}$ (s)	$\tau_{e,coll}$ (s)	$\tau_{i,coll}$ (s)	$\tau_{resistive}$ (s)
LTX	$3.0 \times 10^{-7}$	$6.7 \times 10^{-8}$	$2.9 \times 10^{-6}$	$5.8 \times 10^{-7}$	$2.5 \times 10^{-5}$	$3.3 \times 10^{-1}$
NSTX	$8.2 \times 10^{-7}$	$6.4 \times 10^{-8}$	$2.7 \times 10^{-6}$	$2.0 \times 10^{-6}$	$8.6 \times 10^{-5}$	$2.0 \times 10^1$
DIID-D	$3.9 \times 10^{-7}$	$5.6 \times 10^{-8}$	$2.4 \times 10^{-6}$	$1.6 \times 10^{-5}$	$6.7 \times 10^{-4}$	$2.0 \times 10^2$
ITER	$5.9 \times 10^{-7}$	$1.0 \times 10^{-7}$	$4.5 \times 10^{-6}$	$1.1 \times 10^{-4}$	$4.6 \times 10^{-3}$	$1.3 \times 10^4$

- Distribution function will likely evolve to steady state within a resistive time
- Must consider full time dependence as MHD code time steps (10-100 Alfven times) can be less than the electron collision time

# Hybrid iteration scheme

15



# Status of code

16

- All terms have been implemented
- Good convergence properties observed
  - ▣ See poster #89 on Tuesday afternoon if interested
- Initial benchmarks show good agreement with Sauter analytic formulae for
  - ▣ Neoclassical conductivity
  - ▣ Pressure gradient drive coefficient



# Calculating Sauter-like coefficients

17

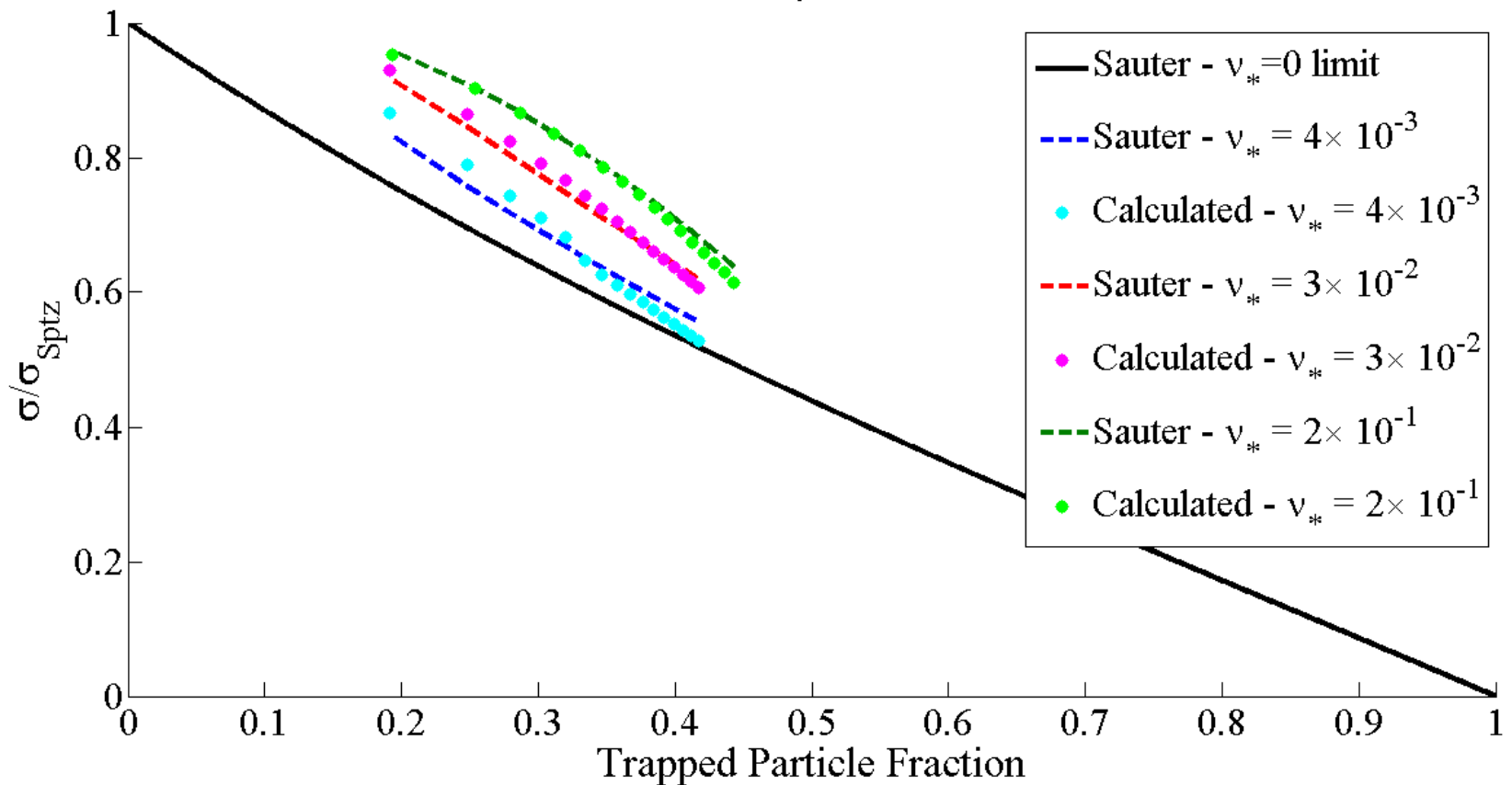
- When run to steady state, we can calculate the neoclassical conductivity and bootstrap current coefficients for an equilibrium
- Must separate inhomogeneous source terms in DKE
- Coefficients given by collisional friction force and pressure anisotropy via parallel Ohm's law

$$\langle \mathbf{J} \cdot \mathbf{B} \rangle = \sigma_{neo} \langle \mathbf{E} \cdot \mathbf{B} \rangle + I \left( \mathcal{L}_{31} \frac{dP}{d\psi} + \mathcal{L}_{32} n \frac{dT_e}{d\psi} \right)$$

# Benchmark with Sauter model (1)

18

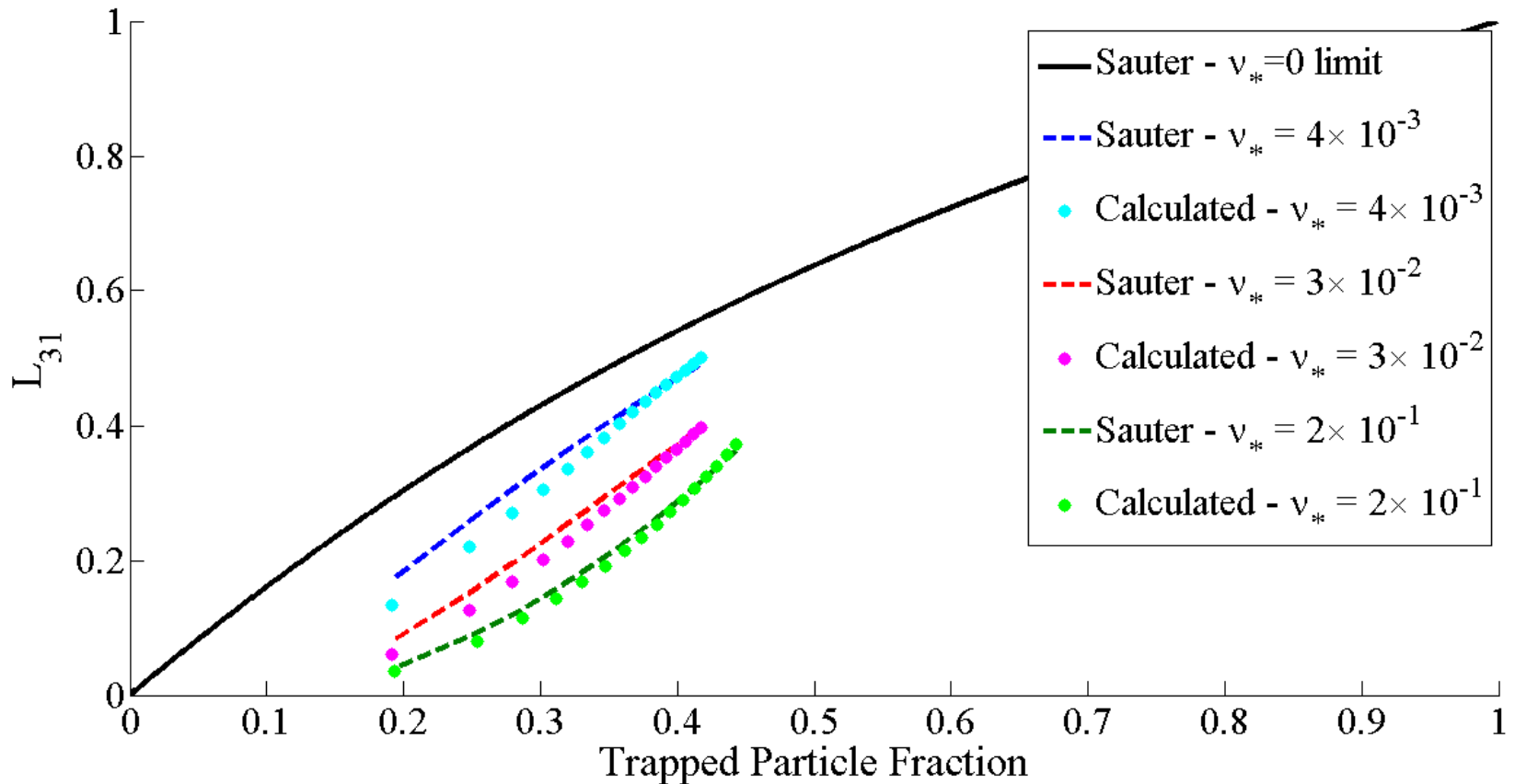
### Conductivity Benchmark



# Benchmark with Sauter model (2)

19

Pressure Gradient Drive Benchmark



# 1D MHD Test Solver

20

□ From  $\mathbf{B} = \nabla\psi \times \nabla\zeta + I\nabla\zeta$   $\frac{\partial\mathbf{B}}{\partial t} = -\nabla \times \mathbf{E}$   $\mathbf{E} + \mathbf{u} \times \mathbf{B} = \mathbf{R}$  , we

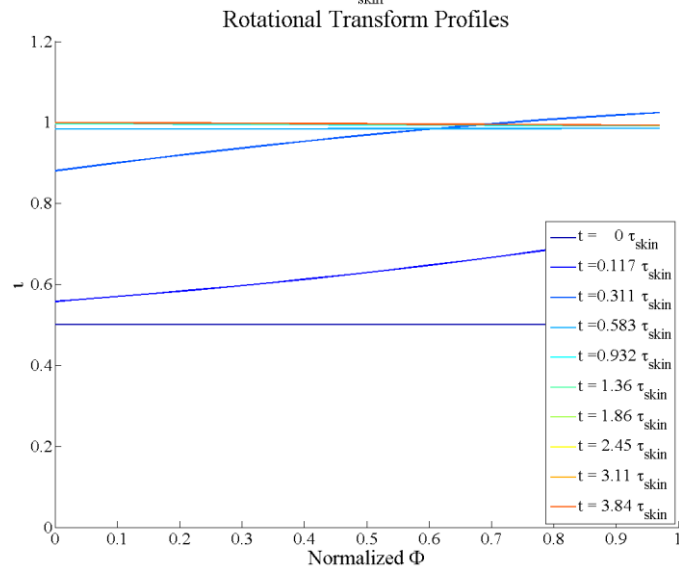
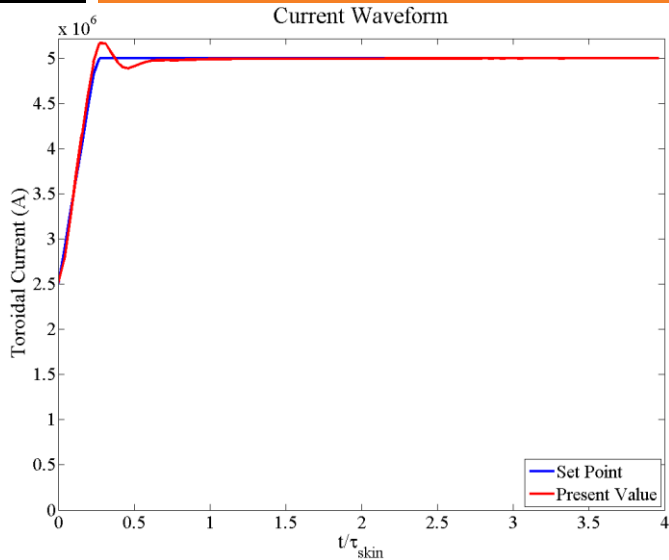
can show that  $\frac{\partial\iota}{\partial t} = -\frac{\partial V_L}{\partial\Phi}$  where  $\Phi = \frac{1}{2\pi} \int \mathbf{B} \cdot \nabla\zeta dV$  ,

$$\iota = -2\pi \frac{d\psi}{d\Phi} , \text{ and } V_L = -2\pi \frac{\langle \mathbf{B} \cdot \mathbf{R} \rangle}{\langle \mathbf{B} \cdot \nabla\zeta \rangle}$$

- Assume a large aspect ratio, expansion equilibrium
- Current controller applies loop voltage at edge
  - ▣ All knowledge of resistivity comes through the Ohm's Law
  - ▣ For stability:  $\mathbf{R} \Rightarrow \mathbf{R}^n + \eta_{Sptz} (\mathbf{J}^{n+1} - \mathbf{J}^n)$
  - ▣ Initial studies do not include bootstrap currents

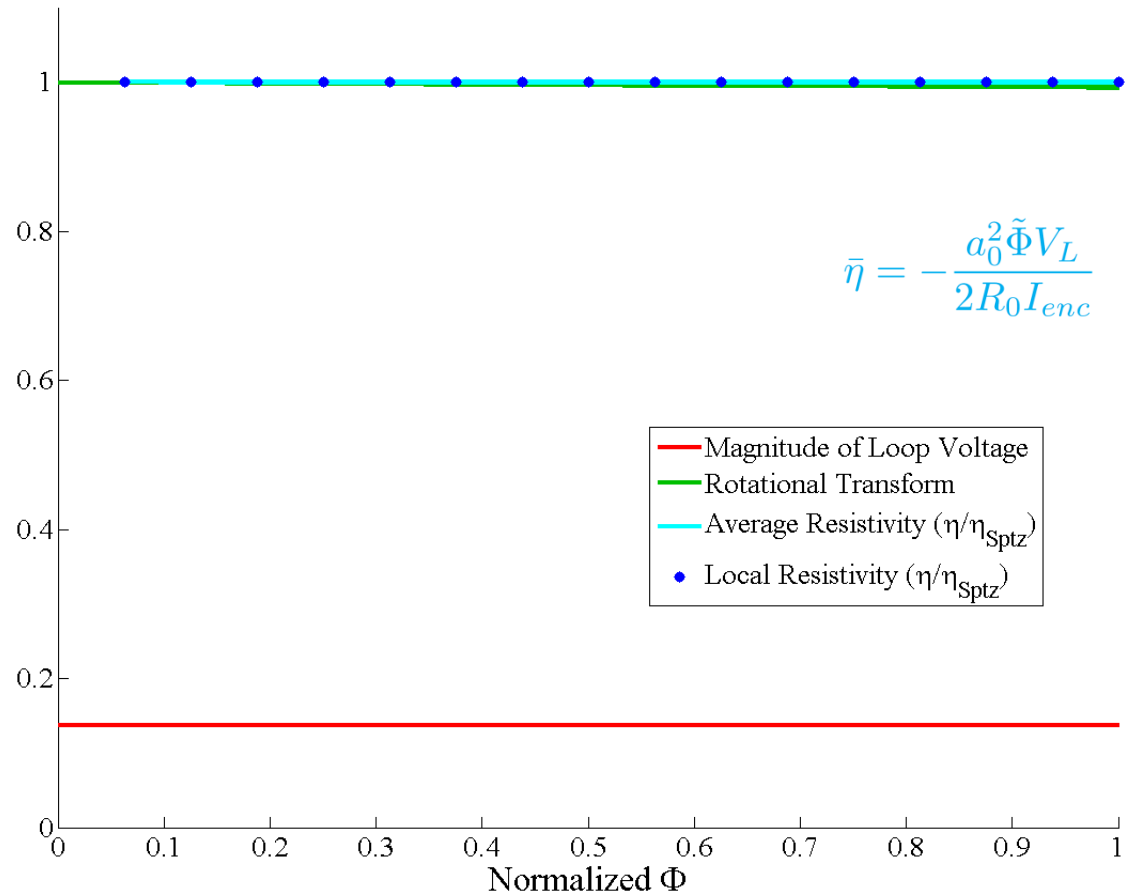
# Evolution with Spitzer resistivity

21



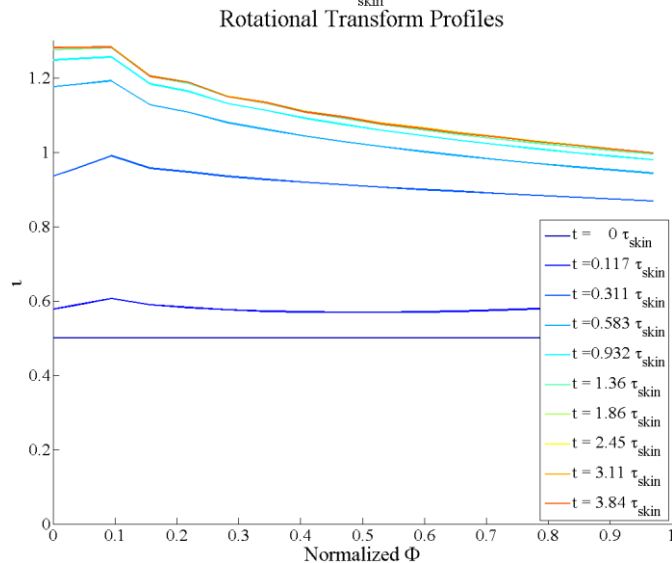
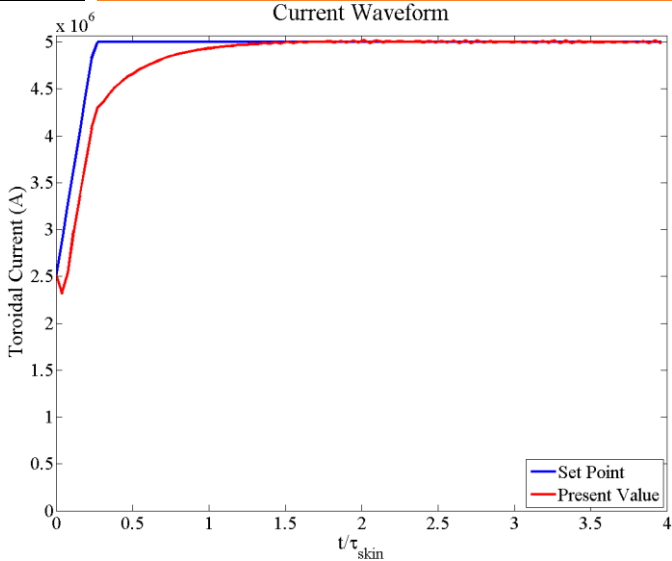
$$\langle \mathbf{B} \cdot \mathbf{R} \rangle = \eta_{Sptz} \langle \mathbf{B} \cdot \mathbf{J} \rangle$$

Profiles at  $t = 3.96 \tau_{skin}$



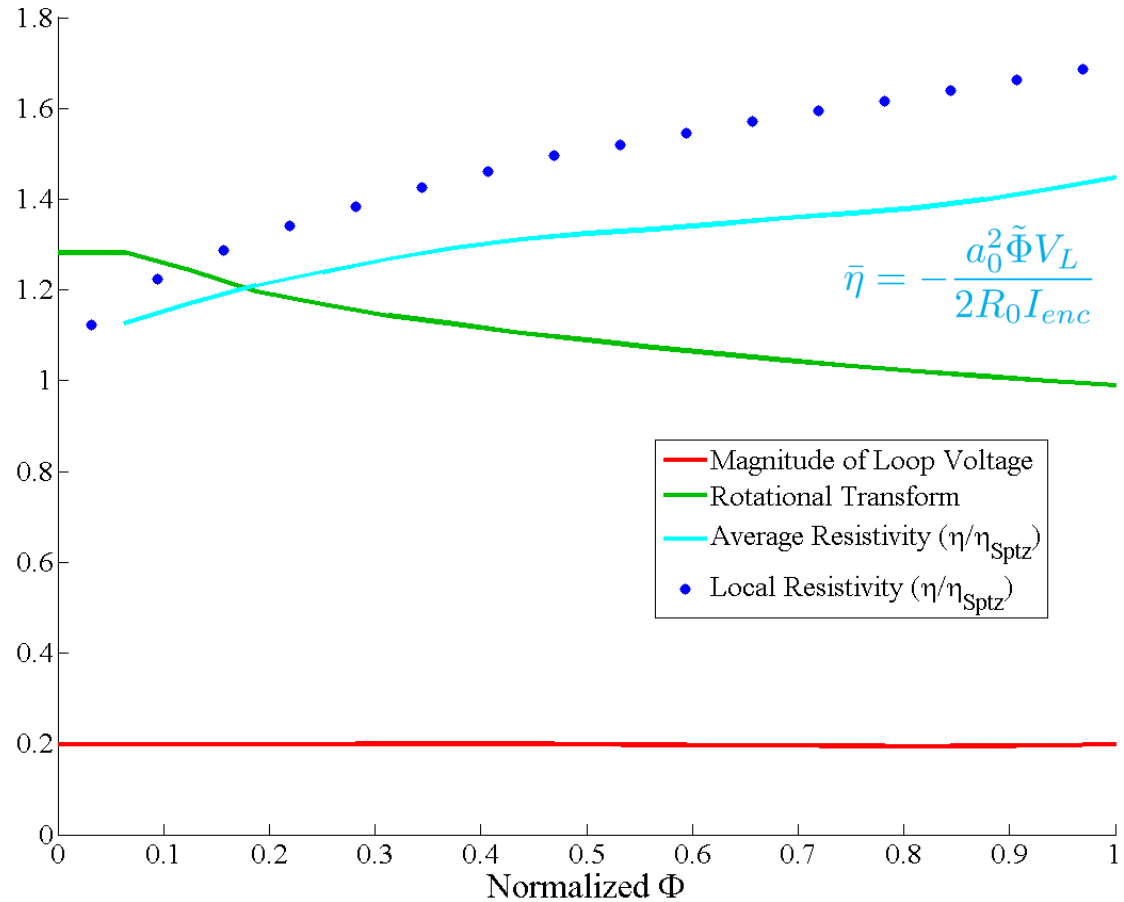
# Evolution with DKE solver (no dP/dψ)

22



$$\langle \mathbf{B} \cdot \mathbf{R} \rangle = \frac{1}{en} [\langle \mathbf{B} \cdot \mathbf{F}_e^{coll} \rangle + \langle (p_{e\parallel} - p_{e\perp}) \mathbf{b} \cdot \nabla B \rangle]$$

Profiles at  $t = 3.96 \tau_{skin}$



# Future work

23

- Complete Sauter benchmark for  $T_e$  gradient drive
- Include bootstrap currents in MHD test solver
- Compare to MHD evolution with Sauter model on different timescales
- Implement separate, but similar, ion DKE solver for ion temperature gradient drive
- Couple to existing, more advanced MHD codes
  - TSC
  - M3D-C<sup>1</sup>
- Investigate alternate representations and extensions to non-axisymmetric geometries

# Summary

- The operation of ITER and other future MCF experiments requires predictive capabilities for core plasma instabilities (e.g., Sawtooths, NTMs)
- To date, no neoclassical code exists that is well-suited for such simulations (work by E. Held excepted)
- We are creating such a code based on the Ramos drift-kinetic formulation
- DKE solution benchmarked to Sauter in steady-state
  - ▣ Temperature gradient coefficient benchmarks coming soon
- Initial hybrid simulations with neoclassical resistivity yield good results
  - ▣ Hybrid simulations with bootstrap current coming soon
- Poster #89 Tuesday afternoon

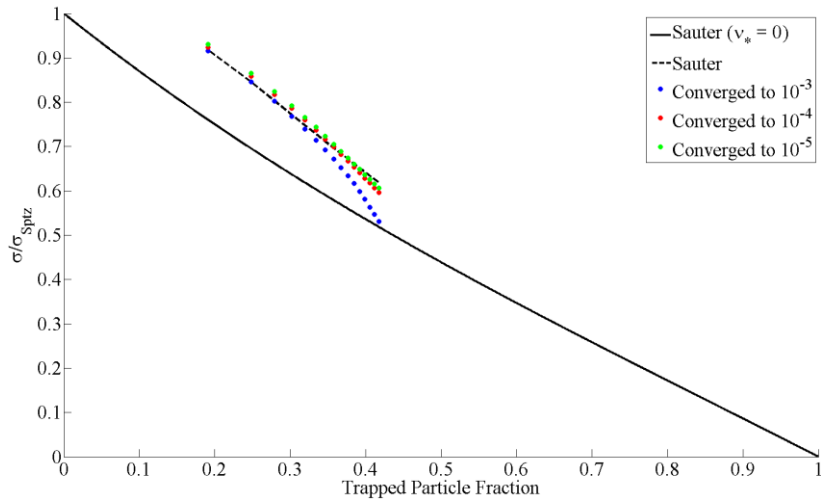


# Extra Slides

# Convergence of Conductivity

26

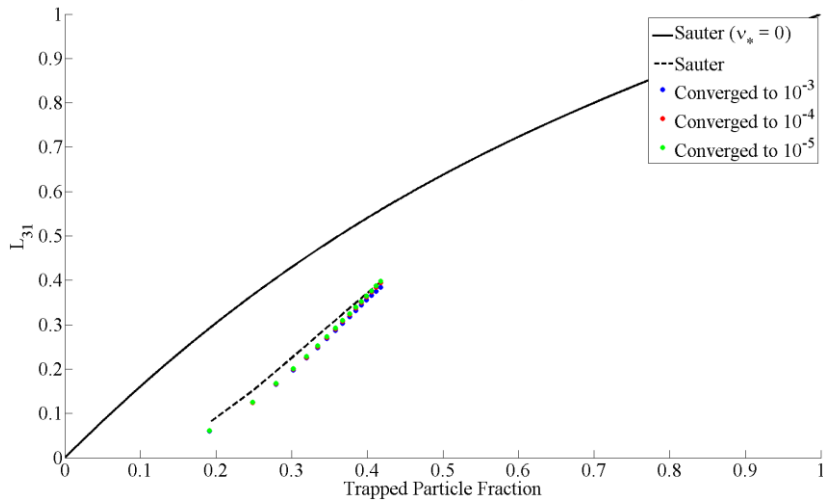
Conductivity at  $v_{*0} = 3.04e-02$



# Convergence of P Gradient Drive

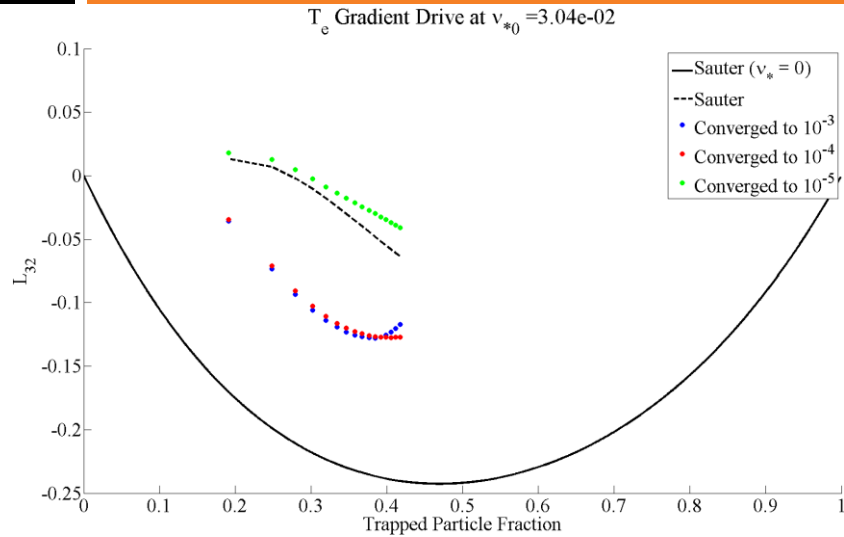
27

Pressure Gradient Drive at  $v_{*0} = 3.04e-02$



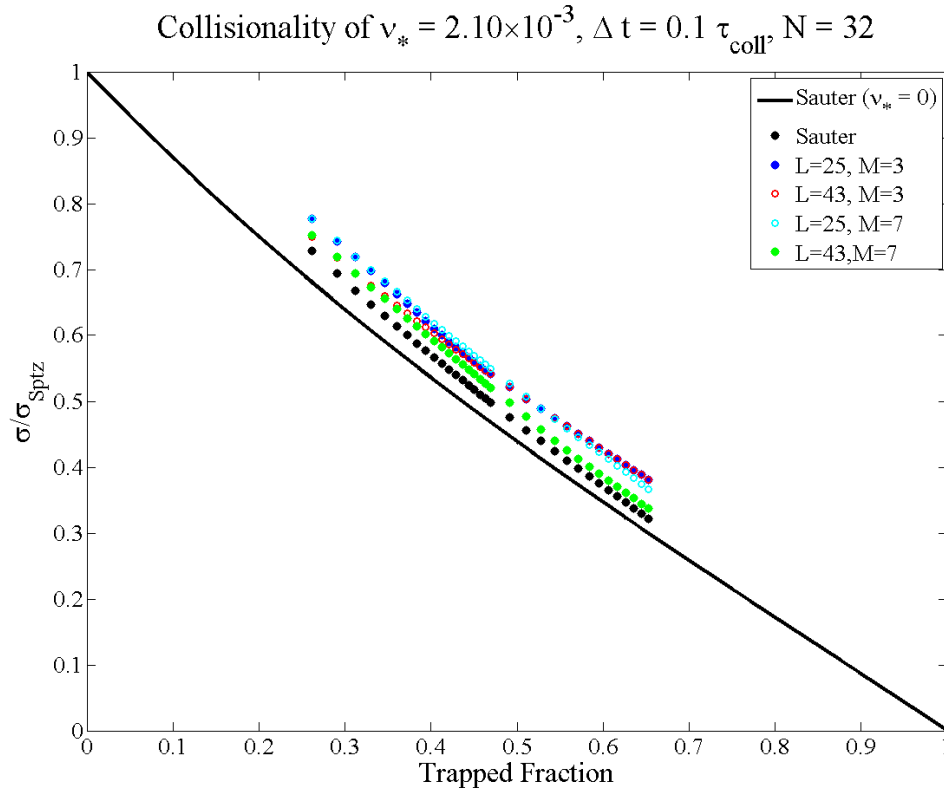
# Convergence of $T_e$ Gradient Drive

28



# Legendre & Fourier Convergence

29



- Low collisionality requires many Legendre polynomials (L) and Fourier modes (M) to converge
- Likely due to steep trapped-passing boundary layer
- May necessitate move to finite element representations